ISSN: 2664-9640

Preparation of flexible transparent piezoelectric nanogenerators and research on electrode materials

Haoen Cheng, Ziqian Wan, Jihao Han, Bingbo Yan

North China University of Science and Technology, Hebei Tangshan 063200, China

Abstract

The preparation process of PZT has always been an important problem of nano-generators, and the nanostructure PZT band is prepared by SOL-GEL method this time, and the etching process is carried out step by step, so that all nanofilms can be stably attached to PZT nanodiames. The following flexible matrix transfer, as a research hotspot in recent years, reacts chemical molecules by heating the flexible matrix. The subsequent etched metal interconnect circuitry and insulating package allow the nanogenerator not to be corroded. In the follow-up, we conducted data experiments on whether the electrode material will affect the output voltage of the piezoelectric nanogenerator and other properties, and concluded that POMs-like materials can meet good electrode requirements, and the electrode packaging of POMs is still under study, and it is hoped that similar inexpensive materials will be used in the future to replace the consumption of special metals.

Keywords

Lead zirconate titanate; Sol-gel method; Flexible matrix transfer; Etching.

1. Introduction

At present, many electronic devices in implantable medical devices use piezoelectric materials, and the use of piezoelectric materials has become a catalyst to accelerate the development of medical devices. After investigation, it was found that PZT has the advantages of large piezoelectric constant, mature production process, high compatibility with the human body, high sensitivity, low price and high performance, but the material of PZT is very brittle and easy to break in a high frequency vibration environment. In order to prevent similar problems, we mix it with composite materials to prepare piezoelectric composites, and geometric configurations can be prepared in energy harvesting chips to achieve the flexibility of PZT piezoelectric chips.

2. Flexible nano piezoelectric equipment production process

The preparation steps of this nano piezoelectric device are: PZT preparation, flexible matrix transfer, etching metal interconnection circuit, and insulated package.

PZT nanofilm preparation

PZT prepares nanostructured PZT bands using the sol-gel method. The overall process is:

First, a 300 nm thick aluminum film is deposited on the substrate, and then the Al2O3 pore film is obtained by an anode corrosion method in the sulfuric acid solution at 20V voltage, and the average diameter of the hole is 25 nm. The layer at the bottom of the Al2O3 pore is removed by the chemical corrosion method of sodium hydroxide solution, and the Au nanowires are prepared in the pores of the porous alumina film by electrochemical method, and connected with the bottom electrode (Ta(20nm)/Au(20nm)/Ta(20nm)) on the silicon substrate to form the bottom electrode of the PZT nanostructured capacitor. PZT membranes with a thickness of 25 and 100 nm were prepared on a silicon-based alumina nanoorder plate medium by sol-gel

ISSN: 2664-9640

spin coating method (coating conditions: 4000 r/min, 40s each time, the concentration of PZT precursors was 0.25mol/L) on a silicon-based alumina nanoordered pore plate medium, and the crystallization treatment of PZT nanodiames was completed at 500 and 600 °C for one hour, respectively.

Next, a mixed solution of HNO3, HCl, and DI is made for etching work, and the solution is heated to 80 °C. The etching work of the Ti electric level can be carried out. After lithography, the photoresist is heated to 110 ° C and baked for another 30 minutes to relieve the oxidation of HNO3.

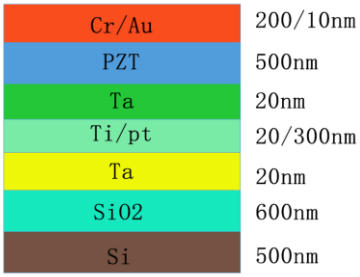

Flexible matrix transfer

The PZT has upper and lower electrodes after transferring the PTZ strip to the flexible matrix. Kapton acts as a flexible matrix and PDMS as an intermediary material.

Prepare a Kapton strip wider than the PZT strip wrap the PZT strip to protect the PZT strip, coat it with a layer of lithographed Kapton adhesive layer, pre-bake for 5 minutes in advance and then heat up to 130 ° C, then lithography and development, and then heat it to 250 ° C so that the chemical molecules of the entire material are fully reacted.

To protect the material it is necessary to coat the material with an 8 μm photoresist to prevent corrosion, and then the SiO2 layer is corroded with a hydrofluoric acid solution at a concentration of 12.5%.

After the corrosion is completed, the photoresist layer is removed with acetone and the silicone is transferred to a layer of silicone on the surface of the material, and the material and the silicone sheet need to be separated from the silicone sheet after repeated confirmation to prevent insufficient contact between the silicone and the material.

The material is then squeezed firmly, in full contact with the kapton layer, and after a few minutes the material is bonded and the silicone stamps are carefully separated.

Finally, a long heating process is carried out in order to polyimide the kapyon layer.

Etch metal interconnect circuits

The electrodes of the material are encapsulated and insulated to prevent the material from shorting during subsequent operations. Note that the depth should be appropriate when connecting the apertures in the RIE strip to ensure the stability of the connection.

Using the ion beam sputtering technique, a layer of Cr with a thickness of 10 nm is plated on the kapton layer, and then a layer of Au 300 nm is plated, and the top electrode and bottom electrode of the PZT layer are connected using Au.

Insulated package

The wire end of the metal interconnection circuit on the material is drawn out of the chip by short-cut alkali-free glass fiber wire, and then the flexible activated carbon fiber line is used to form a linear conductor with a thickness of 30 μm, a width of 270 μm and a spacing of 520 μm at 180 °C.

After the connection, silicone material is used to insulate the wiring part to protect the device from corrosion.

ISSN: 2664-9640

3. PZT nano piezoelectric chip anti-fatigue experiment

The experimental instrument adopts the Swiss RUMUL 250KN high-frequency fatigue testing machine, and the experimental object adopts the prepared PZT nano piezoelectric chip (10mm*5mm).

In order to simulate the working state of the PZT piezoelectric chip on the human face, the flexible PZT nano piezoelectric chip is fixed to the high-frequency fatigue testing machine at different bending angles, and quantitative compression and tensile tests are carried out, and the energy collector detected by the computer is connected to the computer through the wire. The high-frequency fatigue tester will stretch and compress at the distance of L to ensure that the flexible PZT nano piezoelectric chip is still in a bent state after the completion of the stretch. Subsequent compression and stretching at a frequency of 3Hz, and tested at 1mm, 3mm, 5mm, 7mm amplitudes. Each test is 30min. Finally, the voltage output signal of the PZT piezoelectric chip is recorded on the computer terminal, and the energy harvesting performance of the chip is judged.

After 30min of testing, it is necessary to observe whether the intrinsic microscopic characteristics of the PZT nano piezoelectric chip are damaged under a scanning electron microscope, and it is necessary to take pictures and record them.

The flexible PZT nano piezoelectric chip is compressed and stretched according to the frequency of 3Hz, and tested according to the amplitude of 1mm, 3mm, 5mm, 7mm, and no damage to the PZT nano piezoelectric chip has occurred after 30min. Finally, after electron microscopy scanning, the microscopic features of the surface morphology and dislocation defects were not damaged. Microscopic image is shown in Figure 1.

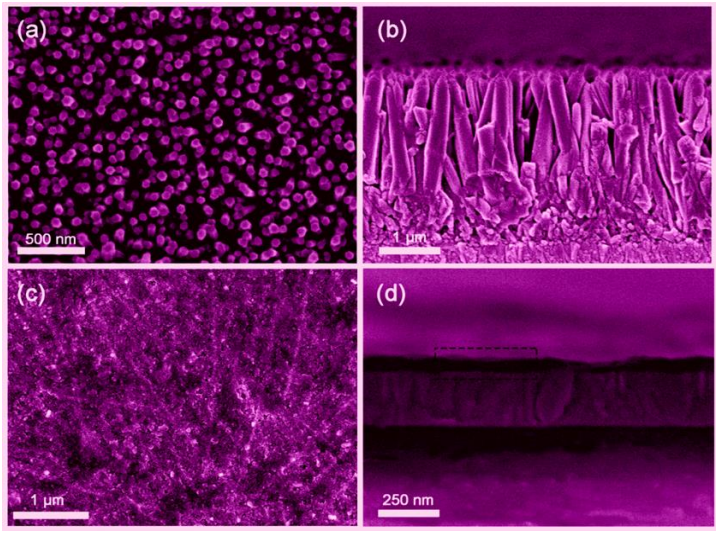

Fig 1: Microscopic eigengraph of PZT nano piezoelectric chip

4. Preliminary experiments on electrode materials for flexible piezoelectric nanogenerators

In this study, three representative Keggin POMs (XM12O40m - where X = P, Si, M = Mo, W) and two Dawson POMs (X2M18O62n - where X = P, M = Mo, W) were selected as the top electrodes to evaluate their effect on the output performance of the nanogenerators and the mechanism of the top electrode during electron transmission. The main reasons for choosing these POMs are as follows. (1) The preparation of POMs electrodes is carried out by spin coating method, these POMs have good solubility in methanol solution; (2) the structure and properties of these POMs remain stable after redox reaction; (3) these POMs have little absorption of visible light.

ISSN: 2664-9640

Figure 2 shows the output current and voltage generated by bending a flexible device to varying degrees. Tables S1 and S2 (online) show the corresponding data. Obviously, the output performance of the same top POM electrode also improves with the increase in bending. Take P2Mo18 as an example, when the bending angle is 15°

At a bend angle of 15°, the output current is 1.2 mA and the output voltage is 0.4 mV. When the bending angle changes from 30° to 90°, the output current and voltage increase from 2.5 mA and 0.9 mV to 8.5 mA and 2.8 mV, respectively. In order to eliminate the interference of the three currents on the PENG, we conducted a switching polarity experiment. When the PENG is connected to the forward, a forward current is generated. When the connection is reversed, the direction of the current also changes. This is the same as the results of the previous literature [42]. As shown in Figure 3, a mathematical model is used to establish the relationship between the output performance and the bending angle, indicating that the output performance is proportional to the bending angle. This is consistent with the results reported in the literature [43].

Figure 2 also shows that the output performance of different POM as electrodes is different at the same bending angle. Devices using SiW12, PW12, PMo12, P2W18, and P2Mo18 electrodes produce approximately 2.4, 2.7, 3.5, 4.9, and 5.3 mA, respectively, at a bend angle of 60°. The output voltage obtained with the electrodes of SiW12, PW12, PMo12, P2W18 and P2Mo18 is about 0.8, 1, 1.2, 1.6 and, respectively

2.4 mV, respectively. Obviously, the output performance is the best when using P2Mo18 as the electrode, and the order of output performance is P2Mo18 > P2W18 > PMo12 > PW12 > SiW12. Interestingly, this output performance trend also applies to other bending angles. At the same time, we also evaluated the cyclic stability of PENG at different frequencies and over long periods of time. Figure 6 shows the output performance of a PEN with P2Mo18 as the electrode at different bending frequencies. At the four frequencies of 20, 10, 5 and 2 s-1, the output performance of the PENG is basically unchanged, Note that PENG has good stability at different frequencies. As shown in Figure 4 (online), there is no significant degradation in output performance after a 1000-second bending cycle. To compare with conventional metal electrodes, we prepared a PENG with Au as the electrode. Figure 5 (online) shows the output performance of using Au as an electrode at different bending degrees. At a bending angle of 15°, the output current is 1.4 mA and the output voltage is0.5 mV。 When the bending angle changes from 15° to 90°, the output current and voltage increase from 1.4 mA and 0.5 mV to 10.5 mA and 0.2 mV, respectively.3.2 mV, respectively. The output performance of PENG with P2Mo18 as the electrode can reach ~80%-90% of the PENG with Au as the electrode. But the cost of POMs composed of rich elements is much lower than the cost of the precious metal Au. The simplicity of the structure and the low cost also make it possible to achieve mass production in the future [15,44].

Several studies have reported that it is feasible to use POMs as the top electrode for nanogenerators. This is because of the energy level relationship between POMs and ZnO. Similar semiconductor properties of POMs were first elaborated by Cham-bers and Hill (1991)[45] and were popularized in their manuscripts. Thus, POMs have a semiconductor-like band structure, which means that when they come into contact with the semiconductor, they can form heterogeneous structures with a rectifier effect [46]. It will facilitate electron transfer and avoid electronic recombination. The rectification effect of the contact surface has been mentioned many times in traditional electrodes, which is also the general operating mechanism of traditional electrodes[12,47,48]. The energy level structure of ZnO and POMs has also been described in many studies [49,50]. Figure 7a shows that the conduction band of ZnO is significantly higher than the LUMO of these Keggin and Dawson POMs, indicating that electrons

ISSN: 2664-9640

may spontaneously inject from ZnO into the LUMO layer of POMs when excited states or polarized charges appear in ZnO.

In addition, the output performance of different POMs as electrodes is inconsistent, which can be attributed to the following aspects: the band structure of POMs is closely related to their own properties and structure. For different types of POMs, the change from Keggin type to Dawson type significantly reduces the LUMO of POMs, indicating that there will be a stronger electron injection tendency between Dawson type POMs and ZnO, as shown in Figure 8. Therefore, in the case of heteroatoms and extra atoms, the output performance of Dawson-type POMs is better than that of Kaijin-type POMs.

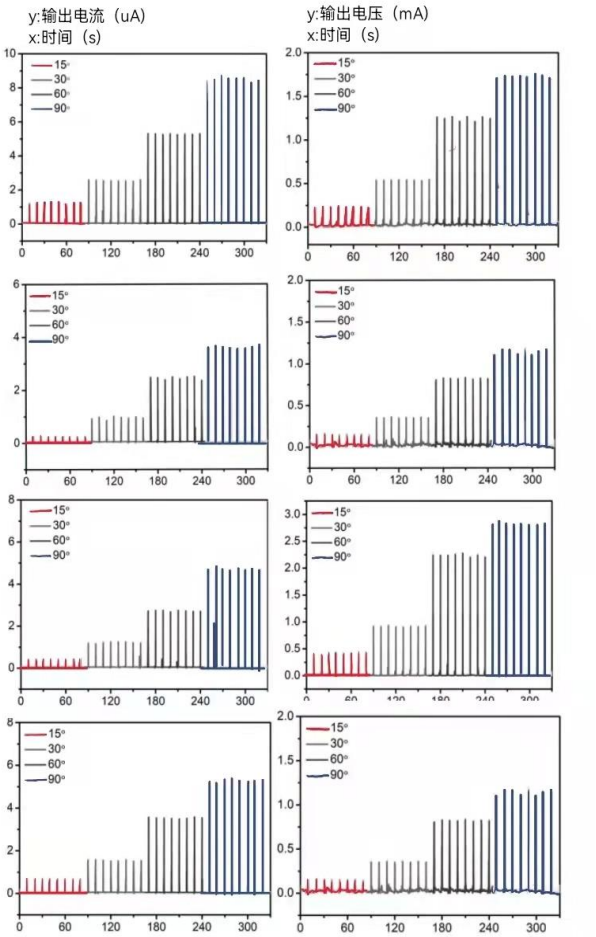

Figure 2. (Color) uses different POMs as the output current (a, c, e, g, i) and output voltage (b, d, f, h, j) of the electrodes at different bends. (a, b) P2Mo18; (c, d) P2W18; (e, f) PMo12; (g, h) PW12; (i, j) SiW12

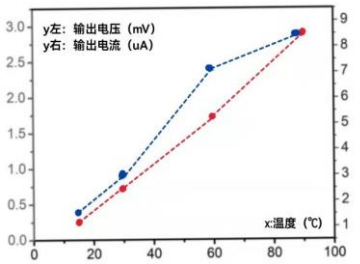

Figure 3. (Color online) The mathematical model between the output performance and the bending degree.

ISSN: 2664-9640

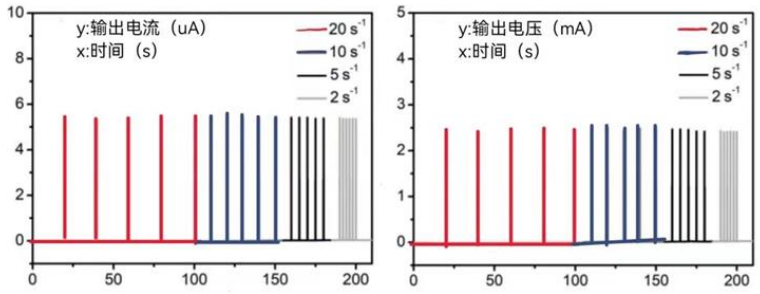

Figure 4. (Color) The output current (a) and output voltage (b) of the PEN with P2Mo18 as the electrode at different bending frequencies.

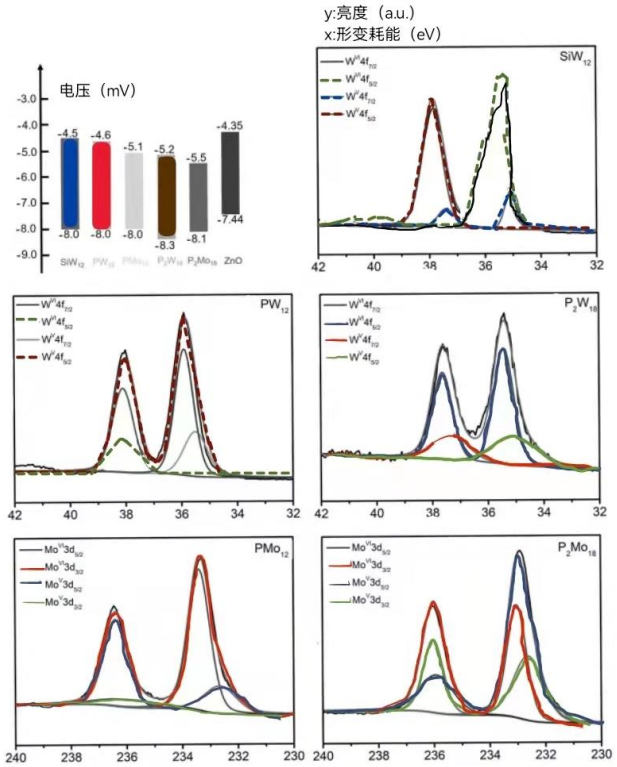

Figure 5. (Color) (a) THE POMs used in this study and the LUMO and HOMO levels and vacuum levels of ZnO. (b)-(d) XpS W 4f core levels are taken from the POM layer as electrodes, including SiW12, PW12, and P2W18, respectively. (e) and (f) at the core level of XPS Mo 3d of the PMo12 and P2Mo18 layers used as electrodes, respectively.

5. Discussion and Results

For the preparation methods, we made a comprehensive analysis and found that compared with the previous preparation methods, there were some problems in our synthesis by chemical methods, and the accuracy of materials would be a problem in sputtering and packaging, so polishing and slicing were necessary steps. However, it is better that the PZT film can be prepared on the silicon-based alumina nanoporous film plate medium to ensure the accuracy. As for etching, it is the main step to ensure the accuracy, and it is also the best method to etch the electrode layer. However, the materials selected for etching have strong oxidizing property, so it is necessary to heat for a period of time after etching to remove the selected chemical solution. However, flexible matrix transfer printing is to make PZT as the main material, which will not be easily damaged by long-term shaking and folding. Finally, the whole

ISSN: 2664-9640

sputtering electrode and insulation package are carried out, and the animal experiment can be carried out after the whole experiment of the energy collector is completed.

Of course, in the previous preparation process, in order to investigate which material replacement has the greatest influence on the conversion efficiency of the energy collector, we adopted basic research and found that the electrode has a great influence on the overall conversion efficiency. Therefore, we have made a basic study on the electrode replacement, and the research sample is ZnO material with better replacement. In order to maintain the corresponding conversion efficiency, we choose to replace it with multi-component mixture, which we call POMs, and the diffraction pattern of its crystal is also more suitable for energy collection caused by folding and tremor. Moreover, compared with gold, it is cheaper in price and simpler in manufacturing process.

Finally, in the face of the problems encountered in the current implanted medical devices, all of them are energy collection. Artificial heart or cardiac vibrator can rely on the powerful organ of the heart to provide energy. However, if it is an implanted organ such as cochlear implant and artificial kidney, it is far away from the heart, and it is inconvenient to install charging equipment or batteries in vitro, so it is necessary to collect energy with the help of muscles and other tremors, and it is also necessary to improve the efficiency of the energy collector. After all, the tremor energy of a dozen muscles may not be higher than that of a heart. As long as the problem of energy collector is solved, the market of artificial implantable medical devices will surely have a great development, even with other remote operations and rehabilitation.

At present, our energy collection equipment lacks some animal experiments, but it has experienced the import and analysis of human face data, which reflects the work efficiency of human face. It has actually proved that human face can indeed generate energy to meet the requirements of cochlear implant equipment, and can realize the perfect charging for 24h. Of course, we still need to consider the use time. We used to bend 50,000 times in 30min with a bending machine, although the bending frequency is high. However, the bending times and various complex tremors in the process of animal experiments will make the material life of the energy collector more demanding, which can at least meet the standard of using in complex environment for about 20 years, which will be our future research direction.

References

[1] Meitl MA, Zhu ZT, Kumar V, et al. Transfer printing by kinetic control of adhesion to an elastomeric stamp [J]. Nature Materials,2006 , 5 (1) : 33 - 38

[2] Chen H, Lu BW, Feng X, et al. Experiments and viscoelastic analysis of peel test with patterned strips for applications to transfer printing ［J］. Journal of the Mechanics and Physics of Solids,2013, 61 (8) : 1737 - 1752

[3] Hwang GT, Byun M, Jeong CK, et al. Flexible piezoelectric thin - film energy harvesters and nanosensors for biomedical applications ［J］. Advanced Healthcare Materials,2015, 4 (5) : 646 - 658

[4] Dagdeviren C, Yang BD, Su Y, et al. Conformal piezoelectric energy harvesting and storage from motions of the heart, lung, and diaphragm [J]. Proceedings of the National Academy of Sciences,2014, 111 (5) : 1927 - 1932

[5] Greenbaum RA, Ho SY, Gibson DG, et al. Left ventricular fibre architecture in man [J]. British Heart Journal,1981, 45(3) : 248 - 263

[6] Cerqueira MD, Weissman NJ, Vasken D, et al. Standardized myocardial segmentation and nomenclature for tomographic imaging of the heart. A statement for healthcare professionals from the Cardiac Imaging Committee of the Council on Clinical Cardiology of the American Heart Association [J]. Circulation,2002, 105(4) : 539 - 542

ISSN: 2664-9640

[7] Schulz DD, Czeczko NG, Malafaia O, et al. Evaluation of healing prosthetic materials polyester mesh resorbable film and collagen elastin matrix / polypropylene used in rabbits abdominal wall defects [J]. Acta Cirurgica Brasileira,2009, 24(6) : 476 - 483

[8] Okuda T, Higashide T, Fukuhira Y, et al. Suppression of avascular bleb formation by a thin biodegradable film in a rabbit filtration surgery with mitomycin C [J]. Graefe's Archive for Clinical and Experimental Ophthalmology,2012, 250(10) : 1441 - 1451

[9] Gupta K, Sivakumar K. Anorexia nervosa and tuberculosis: Case reports and a review of immune mechanisms. International Journal of Eating Disorders 1994;15(3):301-304.

[10] Gonz, Aacute, Lez J et al. Human powered piezoelectric batteries to supply power to wearable electronic devices. International Journal of the Society of Materials Engineering for Resources 2002;10(1):34-40.

[11] Paradiso JA, Hsiao K, Benbasat AY, Teegarden Z. Design and implementation of expressive footwear. IBM Systems Journal 2000;39(3-4):511-529.

[12] Qi Y, McAlpine MC. Nanotechnology-enabled flexible and biocompatible energy harvesting. Energy & Environmental Science 2010;3(9):1275-1285.

[13] Tang QC, Yang YL, Li X. Bi-stable frequency up-conversion piezoelectric energy harvester driven by non-contact magnetic repulsion. Smart Materials and Structures 2011;20(12):125011.

[14] Carrara M, Cacan MR, Toussaint J, Leamy MJ, Ruzzene M, Erturk A. Metamaterial-inspired structures and concepts for elastoacoustic wave energy harvesting. Smart Materials and Structures 2013;22(6):065004.

[15] Ashraf K, Khir MHM, Dennis JO, Baharudin Z. A wideband, frequency up-converting bounded vibration energy harvester for a low-frequency environment. Smart Materials and Structures 2013;22(2):025018.

[16] Roundy S, Leland ES, Baker J et al. Improving power output for vibration-based energy scavengers. IEEE Pervasive Computing 2005;4(1):28-36.